

Tubular Y-Joint Subjected to Axial Loading

Iberahin Jusoh

Department of Mechanical Engineering,
College of Engineering and Islamic Architecture
Umm Al-Qura University, Makkah, Saudi Arabia

Abstract—The typical steel structure that is employed in offshore oil and gas production is usually made of tubular elements assembled using several types of joints. The Y-joint is formed by welding together the brace and chord element at an acute angle. In this paper, the effects of axial load acting on the Y-joint were investigated. Stress concentration factor (SCF) distribution developed around the intersection between the chord and brace is presented. It was found that the maximum SCF of 5.801 occurred at the area of saddle position of the chord under axial load. The finding also indicates that the chord experienced higher SCF as compared to the brace. The results were compared with previous studies and it shows a similar trend of SCF distribution around the Y-joint.

Keywords:- Offshore structure, Y-joint, joint modeling, axial loading, stress analysis

I. INTRODUCTION

Several types of joints may be found in a typical steel jacket structure as shown in Fig.1. Among others, they are Y-joint, K-joint, T-joint as well as K-T-joint. Y-joint is one of a widely used structural member. In this paper, the study focused on the effect of axial loading on the Y-joint. A large number of investigations have been performed on the analysis and design of structural tubular joints [1], [2], [3], [4], [5], [6]. Information related to stress distribution, SCF as well as fatigue strength of a wide range of joint types under various loading conditions was also widely published. Comparison between standard parametric equations and experimental results were compared for T/Y joints [4].

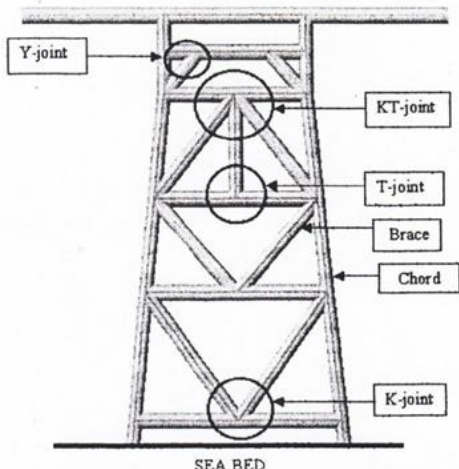


Fig.1. Typical joints on tubular steel structure [6].

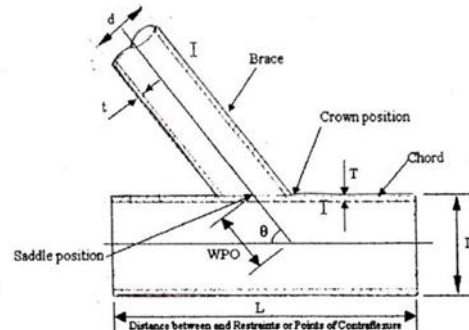


Fig. 2. Description of Y-joint

Finite Element software was used to model the Y-joint and to simulate loading and response due to axial load. Details of the study is presented in the following sections. Geometric notation and non-dimensional parameters describing Y-joints are given in Fig. 2. The basic dimension which describes a simple joint are (1) Chord outside diameter, D, (2) Brace outside diameter, d, (3) Chord wall thickness, T, (4) Brace wall thickness, t, (5) Chord length, (distance between end restraints or points of contra flexure of the chord), L and (6) Length between the brace centreline-chord centreline intersection and the brace centreline-chord surface intersection, WPO. The following non-dimensional geometric parameters are used for the design and assessment of the joint. They are; $\alpha = 2L/D$, $\beta = d/D$, $\gamma = D/2T$ and $\tau = t/T$.

SCF was obtained by performing finite element modeling and analysis of the tubular Y-joint. It related stress distribution around the joint intersection was also determined and presented in the following section. Results from numerical simulation were compared with results obtained from previous studies by Connolly et al [2].

The geometrical parameters adopted in this study are;

Chord diameter, $D = 1.00\text{ m}$
Brace diameter, $d = 0.66\text{ m}$
Chord thickness, $T = 0.0216\text{ m}$
Brace thickness, $t = 0.0197\text{ m}$
Chord length, $L = 3.6\text{ m}$
Brace length, $l = 2.46\text{ m}$

Fig. 3 shows a Y-joint under axial loading. The reference angle is $\phi = 0^\circ$ at the inner side of an acute angle of brace-chord inclination and $\phi = 180^\circ$ for the outer open inclination side as shown.

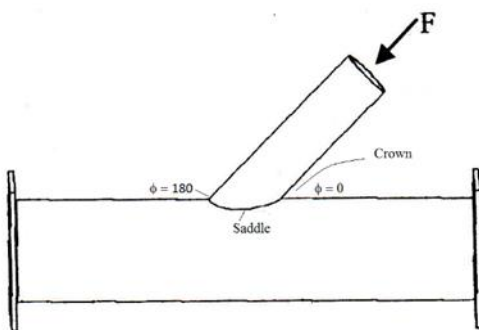


Fig 3. Y-joint subjected to axial load

II. STRESS ANALYSIS OF Y-JOINT

In this study, stress formulation for analysis of Y-joint under axial load was adopted from previous researchers namely Kuang [1], Connolly [2], and Hellier [3], and related stress equations are presented in this section. Several other equations are also being proposed in international standards [7], [8]. The ranges of applicability of the formulae for SCF on the chord and brace of the Y-joint according to Kuang are; $7 \leq \alpha \leq 14$; $0.3 \leq \beta \leq 0.8$; $8.3 \leq \gamma \leq 33.3$; $0.2 \leq \tau \leq 0.8$; $30^\circ \leq \theta \leq 90^\circ$.

Kuang's parametric equations for SCF as a function of joint geometry fitted on both chord and brace sides of the intersection. Combining these two sets of equations the stress distribution for a Y-joint was predicted from its geometric parameters and the mode of loading. The joint was simulated under axial loading of 10 kN. The following equations denote the SCF as a function of joint geometry for chords and brace. SCF for Y-Joint subjected to axial loading [1];

$$\begin{aligned} SCF_{Chord} &= 1.981\alpha^{-0.057}e^{-1.2\beta^3}\gamma^{0.808}\tau^{1.333}\sin^{1.694}\theta \\ SCF_{Brace} &= 3.751\alpha^{0.12}e^{-1.35\beta^3}\gamma^{0.55}\tau\sin^{1.94}\theta \end{aligned} \quad (1)$$

Connolly [2], has conducted a systematic study of stresses in tubular Y-and T-joints for thin-shell finite element analyses. The analysis covers a wide range of joint geometries under axial loading. For each mode of loading, and for both chord and brace sides, the results of this study were used in deriving characteristic formulae for the stress distributions around the intersection. The SCF values presented are those obtained at the intersection line of the mid-surface between the brace and chord. For all the axial loading cases, the chord end conditions were taken as simply supported.

The limit of applicability of Connolly's UCL equations are as follows;

$$\begin{aligned} 6.21 \leq \alpha; 0.2 \leq \beta \leq 0.8; 7.6 \leq \gamma \leq 32.0; 0.2 \leq \tau \leq 1.0; \\ 35^\circ \leq \theta \leq 90^\circ \end{aligned}$$

Chord: for $\phi = 0^\circ$

$$\begin{aligned} SCF_C^0 &= 0.575\alpha^{-0.063}\beta^{-0.2070^{1/2}}\tau^{(0.988-0.133/\theta)} \\ &\times \exp(0.665\beta^5 + 0.0204\gamma + 1.64\sin\theta - 0.469\beta\tau) \end{aligned} \quad (2)$$

Chord: for $\phi = 180^\circ$

$$SCF_C^{180} = 3.845\alpha^{0.039}\beta^{-0.105\theta}\tau^{(0.906-0.055/\theta^3)} \quad (3)$$

Brace: for $\phi = 0^\circ$

$$\begin{aligned} SCF_C^0 &= 1.46\alpha^{0.0098}\beta^{0.214/\theta}\tau^{(0.623-0.081\theta\tau^2)} \\ &\times \exp\left(0.872\beta^2 - 0.00104\gamma^2 + 1.47\sin\theta + \frac{0.0004\gamma^2}{\beta} - 1.73\beta\tau\right) \end{aligned} \quad (4)$$

Brace: for $\phi = 180^\circ$

$$\begin{aligned} SCF_C^{180} &= 19.05\alpha^{0.035}\beta^{(\frac{0.213}{\theta}-0.0439)}\tau^{(0.48+0.0089/\theta^2)} \\ &\times \exp\left(-0.00148\gamma^2 - 1.25\sin\theta + \frac{0.00055\gamma^2}{\beta} - 1.09\beta^2\tau\right) \end{aligned} \quad (5)$$

The results were found to have good agreement in most cases and the formulae were also found to be conservative. In Connolly's load cases, the equations for hot-spot SCF were generally overestimating the measured SCFs from steel model tests. Thus, it is said that the equations are the most reliable in predicting a conservative value of SCF which could be used in design [2].

III. RESULTS AND DISCUSSION

The distribution of SCF along the chord-brace intersection is presented in TABLE 1 and plotted as shown in Fig. 4. The crown position with $\phi = 0^\circ$ at the inner inclined angle between the brace and chord is previously defined. The results of the axial loading give rise to the higher SCF at the chord member as compared to SCF on the brace. The location of the maximum hot-spot stress value is at the saddle position of the joint at an angle of about $\phi = 100^\circ$. It is expected the location is where the geometrical of chord elements at almost horizontal to axial load from the brace thus experiencing maximum compression force that gives rise to maximum equivalent stresses. The stress magnitude contour is presented in Fig. 5. Maximum SCF magnitudes occurred along the saddle point indicating that the related maximum strain also occurred at that location. With these SCF distributions, elements at the joint intersection experienced maximum deformation and hence stress level as shown in Fig. 4. Maximum magnitude of SCF = 5.801 occurred at the saddle region where $\phi = 100^\circ$.

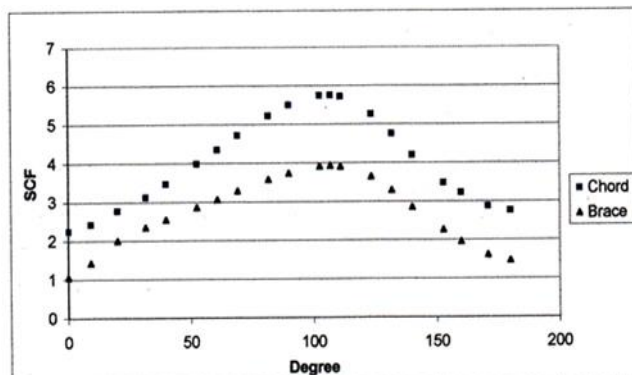


Fig 4. Chord-brace intersection SCF distribution

TABLE 1: Distribution of SCF along the welded Y-joint

Location ϕ (deg)	SCF value	
	Chord	Brace
0	2.250	1.005
10	2.436	1.375
20	2.812	2.001
30	3.125	2.304

40	3.500	2.578
50	3.990	2.879
60	4.389	3.043
70	4.752	3.250
80	5.211	3.602
90	5.503	3.750
100	5.801	3.916
110	5.799	3.900
120	5.276	3.650
130	4.800	3.251
140	4.175	2.899
150	3.615	2.387
160	3.256	1.895
170	2.913	1.675
180	2.890	1.445

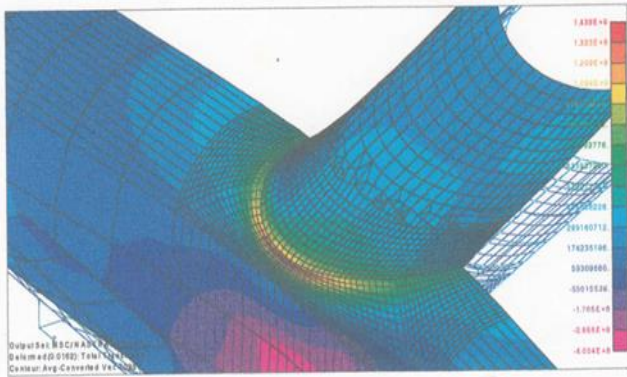


Fig. 5. Stress contour for tubular Y-joint.

Fig. 6 and Fig. 7 show a comparison between simulation results and a previous study by Connolly using UCL-equations. It is clear that the results of this study are in good agreement with results from a previous study [2] for the Y-joint under axial loading as shown in Fig. 6. The results show the SCF distribution for chord and brace respectively showing similar trends. The difference in magnitude of SCF can be due to the effect of assumptions in the modeling and loading considered in the analysis and simulation. However, slight differences appeared for the distribution of SCF for brace elements with this study giving a maximum value of 4.90 as compared to 6.35 by Connolly's UCL-equation as shown in Fig.7.

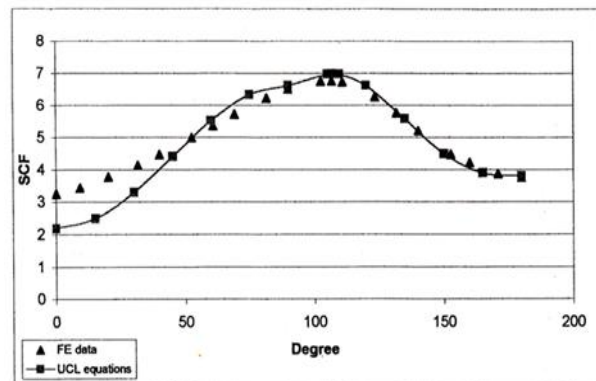


Fig. 6. Chord's SCF distribution from FEM data and UCL equation.

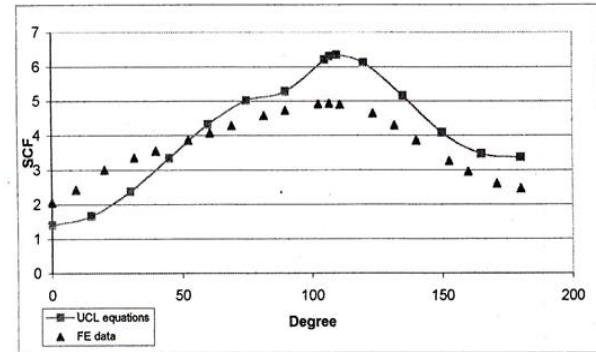


Fig. 7. Brace's SCF distribution from FEM data and UCL equation

Connolly [2] stated that their results from the empirical equations used in the analysis are rather overestimated values of SCF at the joint as compared to their experimental values. The differences shown in Figs. 6 and 7 are therefore of acceptable magnitudes. The point of maximum SCF occurred at the saddle region of the joint, hence, the member's elements experiences the maximum induced stress. Maximum deformation of the joint should be expected at the point with maximum stress.

IV. CONCLUDING REMARKS

The results obtained from the stress concentration factor study on the Y-joint model can be summarized as the following.

Maximum stresses experienced by joint elements occurred at the saddle region near the intersection weld, $\phi = 100^\circ$. The distribution of stresses in the vicinity of the chord-brace intersection is influenced by the member's geometrical shape as well the direction of loads. The chord at the saddle region under axial compressive load experienced maximum stresses. These local maximum stresses give rise to the maximum elemental deformation. Local stresses near the saddle weld intersection are much higher than the nominal stresses of the chord and brace. The results of the simulation study show a good agreement with the results of those theoretical methods.

REFERENCES

- [1]. J.G. Kuang, A.B. Potvin, and R.D. Leich. 'Stress concentration in tubular joints', Society of Petroleum Engineers, 1977.
- [2]. M.P. Connolly, A.K. Hellier, W.D. Dover, and J. Sutomo. 'A parametric study of the ratio of bending to membrane stress in tubular Y- and T-joints', International Journal of Fatigue, Vol. 12 No 1, 1990. pp 3-11.

- [3]. A.K. Hellier, M.K. Connolly, and W.D. Dover. 'Stress concentration factors for tubular Y- and T-joints', International Journal of Fatigue, Vol. 12 No 1, 1990. pp 13-23.
- [4]. P. Thibaux and S. Cooreman, Computation of stress concentration factors for tubular joints, Proceeding of the ASME 2013 32nd International Conference on Ocean, Offshore and Arctic Engineering, OMAE2013-10934, 2013 Nantes, France.
- [5]. S.T. Lie, T. Li, and Y.B. Shao, Stress intensity factors of tubular T/Y-joints subjected to three basic loading, Advance Steel Construction, Vol.12, No.2, 2016, pp109-133.
- [6] I. Jusoh. 'In-Plane Bending and SCF of Tubular Y-Joint', SSRG - International Journal of Mechanical Engineering, Vol. 6, Issue 12, Dec 2019.
- [7] API RP-2A, (American Petroleum Institute) Recommended Practice for Planning, Designing and Constructing Fixed Offshore Platforms- Working Stress Design API RP 2A-WSD, 2010.
- [8] DnV RP C203 (Det Norsk Veritas), Fatigue Design of Offshore Structures", Norway. 2010